IOSR Journal of Applied Geology and Geophysics (IOSR-JAGG)
e-ISSN: 2321–0990, p-ISSN: 2321–0982.Volume 9, Issue 3 Ser. I (May – June 2021), PP 15-27
www.iosrjournals.org

A new occurrence of yttriumuraninite, Selenium minerals, Sphalerite and Pyrite assemblages from research drilling at Abu Rusheid uranium mineralization, southern Eastern Desert, Egypt.

Ahmed S. Shalan
Nuclear Materials Authority, P.O. Box: 530, El-Maadi, Cairo, Egypt.

Abstract
Based on petrographic investigation applied to the picked core samples through pre-pilot drillhole north of Wadi Abu Rusheid, SED, Egypt with depth of 47m which have been studied perfectly, the subsurface metamorphic sequence are (from top to bottom): mica schist, buffish gray mylonitic gneiss, quartz feldspar whitish mylonitic gneiss, caverneous mica schist, quartz-hornblend-biotite schist and finally whitish gray mylonite gneiss interrupted by thin layer of quartz-carbonate-hornblend-biotite schist. Mineral association found for the first time in the area under investigation, the yttriumuraninite (gummite), uranophane, are found together with botryoidal sphalerite (with colloform texture), Przibramite ((Zn,Cd)S), Clausthalite (PbSe) and Berzelianite (Cu_2Se) as well as well-developed pyrite that confirmed by Scanning Electron Microscope (SEM). Thorite and uranothorite are also predominant primary radioactive minerals in the studied borehole. Uranophane and Kasolite are the uranium secondary mineral more abundant. Other radioelements-bearing minerals were recorded such as Betafite [$(Fe,Ca,Th,U)(Ti,Nb,Ta)O_6$-·$nH_2O$], samarskite ($YFe^{3+}Fe^{2+}U,Th,Ca)_2(Nb,Ta)_2O_8$, fergusonite (Nb, Y, Ta, U, Al, Mg, Fe, REE) and zircon. The dominantly associated of their minerals are xenotime, monazite, fluorite, and opaques, this mineralization with epigenetic contribution by circulating hydrothermal solutions illustrates by the presence of colloform textures. The radiometric analysis revealed that, the whitish gray mylonitic gneiss samples represent the highest radioactive zone, where the eU ranges from 68 to 179 ppm with an average 147 ppm and the eTh content varies from 155 to 467 ppm with an average 253ppm. The (eTh/eU) ratio ranged from 0.9 to 2.8 with an average 1.8 as well as thorium content at this zone represents the highest thorium content along the borehole while the schistose rock types represent the lowest values along the studied borehole in addition to there is a general trend for increasing of uranium and decreasing thorium with depth for the studied borehole.

Keywords; *pre-pilot drillhole, Mylonitic gneiss, Gummite, Przibramite, Clausthalite, Abu Rushied. Egypt.*

Date of Submission: 02-05-2021 Date of Acceptance: 16-05-2021

I. Introduction

Natural uranium-bearing phases have highly variable chemical composition (Frondel, 1958; Xu et al. 1981). They occur as: (a) simple oxides such as uraninite, pitchblende and their altered product - gummite; (b) silicates like coffinite, zircon and allanite; (c) complex (multiple) oxides like brannerite (U-Ti complex), davidite, fergusonite, samarskite and betafite; and (d) phosphates like xenotimeand monazite. At shallow depths and at the surface the uraninite is completely replaced by gummite which penetrates the silica and uranophane shells along radial expansion cracks (Whittle 1960). Gummite is a vague term that has been and is used in various ways. Probably its commonest present-day use is as a generic term for gumlike or dense fine-grained pseudomorphic alteration products of uraninite (Lang, 1962). Abu Rusheid mylonitic gneisses host economic deposits of HFSE (Nb, U, Th, Zr, HREE and Y) in addition to base metals (Pb, Zn and As). The exploration efforts, carried out by the Nuclear Materials Authority of Egypt (NMA) at Abu Rusheid area, led to the discovery of the uranium mineralization at some shear zones occur within mineralized mylonitic gneissic rocks and at the thrust plane between ophiolite mélange and these rocks. Agoal of the Abu Rusheid Scientific drilling program is to explore the uranium mineralization and associated economic minerals at deeper levels and also to obtain more subsurface geological data of Abu Rusheid area. This study is concerned with the subsurface geology, petrology and mineralogy of the core samples recovered from shallow pre-pilot drillhole.

II. GEOLOGIC SETTING

A) Surface Geology. The Egyptian Eastern Desert, Sudan, western Saudi Arabia, Ethiopia, Eritrea, Jordan and Yemen belong to the so-called Arabian Nubian Shield, which is characterized by four main rock sequences: (i) an island arc assemblage; (ii) an ophiolite assemblage; (iii) a gneiss assemblage that comprises the core

complexes; and (iv) granitoid intrusions (Abd El-Naby et al., 2000; Abd El-Naby and Frisch, 2002 and 2006). Sikait-Nugrus-Abu Rushied areas at South Eastern Desert (SED) are representing the southeastern sector of the Hafafit metamorphic complex. It occupies high-grade infrastructural rock assemblages, which are represented by metamorphic volcano-sedimentary series, quartzo-feldspathic gneisses of tonalite and granitic composition, and amphibolites (Fig. 2). They are overthrusted, via the Nugrus thrust zone by an obducted ophiolitic mélange. This mélange represents the supra-structural assemblage and consists of large nappes obducted over the infrastructure (Kroner et al., 1987). These rock associations are intruded by intracratonic gabbroic and granitic rocks (Saleh, 1997; Assaf et al., 2000; Ibrahim et. al., 2004. and Mahmoud, 2009). Abu Rusheid-Sikait area is located at the Southern part of the Eastern Desert of Egypt, about 45 km to the Southwest of Marsa-Alam city (Fig. 1). It occupies approximately 73.5 km^2. It is bounded by Latitudes 24° 36′ 43" and 24° 38′ 26" N and Longitudes 34° 46′ 00" and 34° 46′ 35" E. Abu Rusheid-Sikait area is bordering to the major shear zone known as the Nugrus thrust fault (Greiling et al., 1988) or the Nugrus strike-slip fault (Fritz et al., 1996) and/or Sha'it–Nugrus shear zone (Fowler and Osman, 2009). Abu Rusheid–Sikait granitic pluton elongated in NW-SE and thinning in NE-SW. Abu Rusheid area is located between a major thrust to the NE and aminor one to the SW. Semi-detailed geologic map of Abu Rusheid mylonitic gneiss and surrounding rocks was prepared out based on field relations and structural observation (Fig. 1). The main rock units encountered in this area are grouped as follows; - (a) Gneissic rocks, (b) Opiolitic mélange, (c) Granitic rocks, (d) Post-granitic dykes and veins. The gneissic rocks occur in the field down thrusted the ophiolitic mélange and foliated in ENE-WSW direction. The Lithologic contacts with ophiolitic melange, where exposed, are tectonized and well defined (Fig. 2a). These rocks occupy the core of the granitic pluton and cross cut by three shear zones; the first two zones extend NNW-SSE, while the third extends ENE-WSW. The study area is characterized by low to moderate topography and highly tectonized rocks. Gneissic rocks are characterized by containing mineralization as uranium and associated minerals. The ophiolitic mélange, consisting of ultramafic rocks and layered metagabbros set in metasedimentary matrix. The latest Pan-African activity in the mapped area is represented by a suite of leucogranites, pink granites and post-granitic dykes, veins and pegmatitic body. The younger granites are locally developed along thrust faults and containing numerous enclaves from older rocks particularly mica schist. Several masses of these granites are found in Wadi Nugrus-Abu Rusheid. The granitic rocks occupy the major part of the mapped area and represented from the NW direction by porphyritic biotite granites followed by deformed biotite granites and two mica granites, whereas the muscovite granites occupy the SE part of the pluton (Ibrahim et al., 2004).

According to the discovery of some surfacial uranium mineralization at the studied area (Ibrahim et al., 2002 and 2004), and depending on ground geophysical surveys which were conducted to explore the mineralized zones at depth and detailed surface geology, diamond core drilling project are carried out to complete the information about the uranium mineralization at Abu Rushied area. It was suggested by NMA work team in Abu Rusheid project to obtain more geological and mineralogical data of subsurface

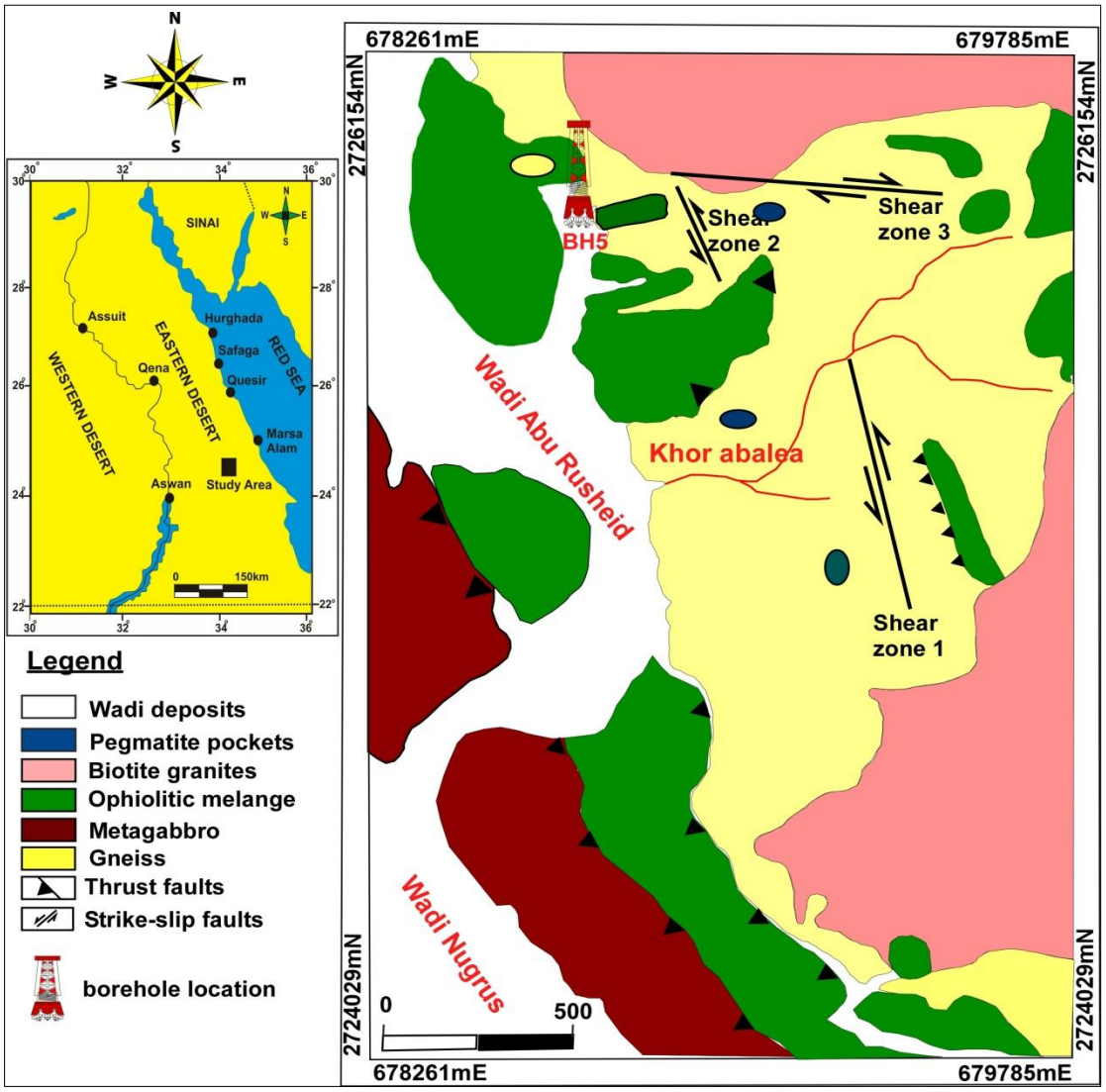

Fig. (1): Geologic map of Abu Rusheid area showing location of the studied borehole, SED, Egypt, after Ibrahim et al., 2004.

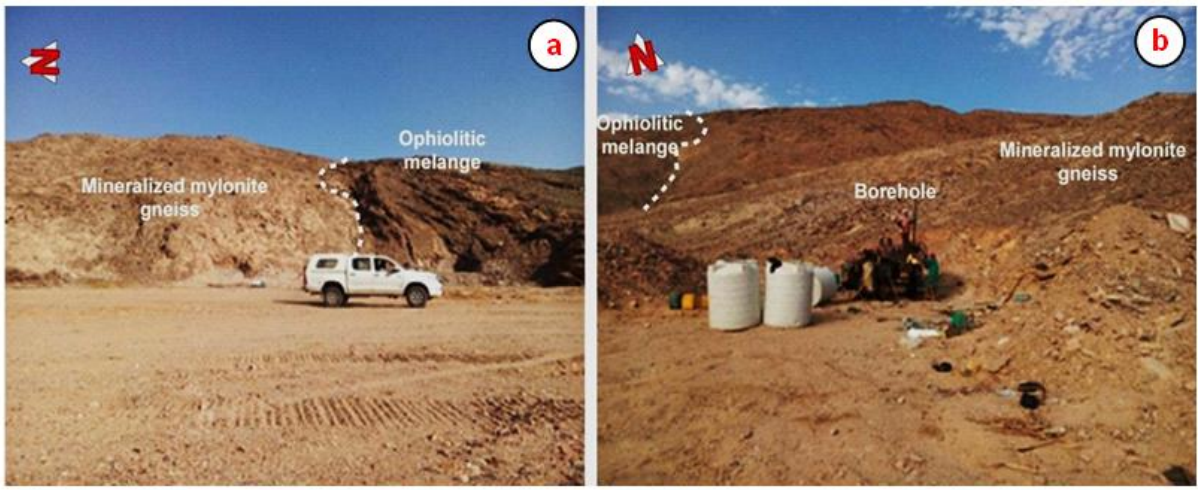

Fig 2a- Ophiolitic melange thursted over mylonitic gneiss, Abu Rusheid area, SED, Egypt.
Fig. 2b- Drilling rig at the studied borehole, north Wadi Abu Rusheid area, SED, Egypt.

B) Sub-surface geology of Abu Rusheid mylonite gneissic rocks north Wadi Abu Rusheid

anomalies. The drilling activities during season 2019-2020 At Abu Rusheid uranium occurrence comprise one drillhole had been drilled to 48m depth to check the radioactive mineral associations with depth (Fig. 2b). This borehole is vertical (90°) and it had been drilled to about 48m depth from the topographic level. The main target for that borehole is to characterize the behavior and distribution of uranium mineralization and associating economic minerals at deeper levels.

The lithostrtigraphic metamorphic sequence is constructed for the studied borehole based on the morphological features and petrographical examination, (Fig. 3). It is clear that the subsurface units are lithologically represented mainly (from top to bottom): mica schist, buffish gray mylonite gneiss, quartz feldspar whitish mylonite gneiss, caverneous mica schist, quartz-hornblend-biotite schist and finally whitish gray mylonite gneiss interrupted by thin layer of quartz- carbonate-hornblend-biotite schist. The detailed field description of core samples picked from the studied borehole will be briefly discussed.

Mica schist is characterized by black color; fine to medium grained, directly overlies the quartz feldspar white mylonitic gneiss with sharp contact (Fig. 4a). The thickness of this unit doesn't exceed 20 cm. The buffish gray mylonite gneiss core samples are massive rock characterized by buffish gray color, moderately to strongly foliated and regular grain size ranges between medium to fine with gneissose structure (Fig. 4b). The foliation is defined by flattened biotite-rich streaks and indistinct, elongated lithosomes of quartz and feldspar and invaded by numerous thin pegmatite veinlets (Fig. 4c). The buffish gray mylonite gneiss is extending from 1m to 21m dissected sometimes with pegmatite lenses and intercalated with different types of schists and gneisses. It is highly fractured and sheared, that filled by iron oxides and also shows signs of brecciation along some fractures (Fig. 4d). The quartz feldspar whitish mylonite gneiss occurs in four thin layers along the borehole, composed mainly of quartz and feldspar with white color reflects very little amount of mica minerals. Staining with iron oxides is observed along some core samples (Fig, 4e). The Quartz-hornblende-biotite schist core samples are mainly hard and compacted, characterized by schistose structure and black color with variable degrees, medium- to fine-grained (Fig. 4f). It present as one band sandwiched by the buffish gray mylonitic gneiss marked by sharp contact and mainly composed of quartz, hornblende and biotite with schistose structure, reaching about 0.5 m in thickness (see fig. 3). Finally, the whitish gray mylonite gneiss is present as two bands; the first is estimated as 1m thickness, extends from 15.7m depth to 16.85m depth that characterized by light gray color, high foliation and low sulphide content (Fig. 4g), underlain by thin layer of caverneous mica schist with sharp contact (Fig. 4h), and the second as 26m thickness, extends from the 21m depth to nearly the bottom of the borehole (see fig.3), characterized by whitish gray to dark gray color and grain size ranges between medium to fine with gneissose structure (Fig. 4i). It is also dissected by pegmatite lenses (Fig. 4j). Secondary uranium mineralization was recorded as orange and yellow amorphous material along some horizontal fracture planes associating with iron oxides at the distance starting from 21m depth to 23m depth in the studied rock (Fig. 4k). Pyrite and sphalerite are the main sulphide minerals encountered in the second band as disseminations in the studied samples with high amount, easily recognized with naked eye or by hand lens (Fig. 4l). The quartz-carbonate-hornblend-biotite schist zone represents by one band sandwiched also by whitish gray mylonite gneiss with sharp contact (Fig. 4m) and extends from 40.6m depth to 42m depth with thickness about 1.5m. It is composed mainly of quartz, carbonate and mica with schistose structure (Fig. 4).

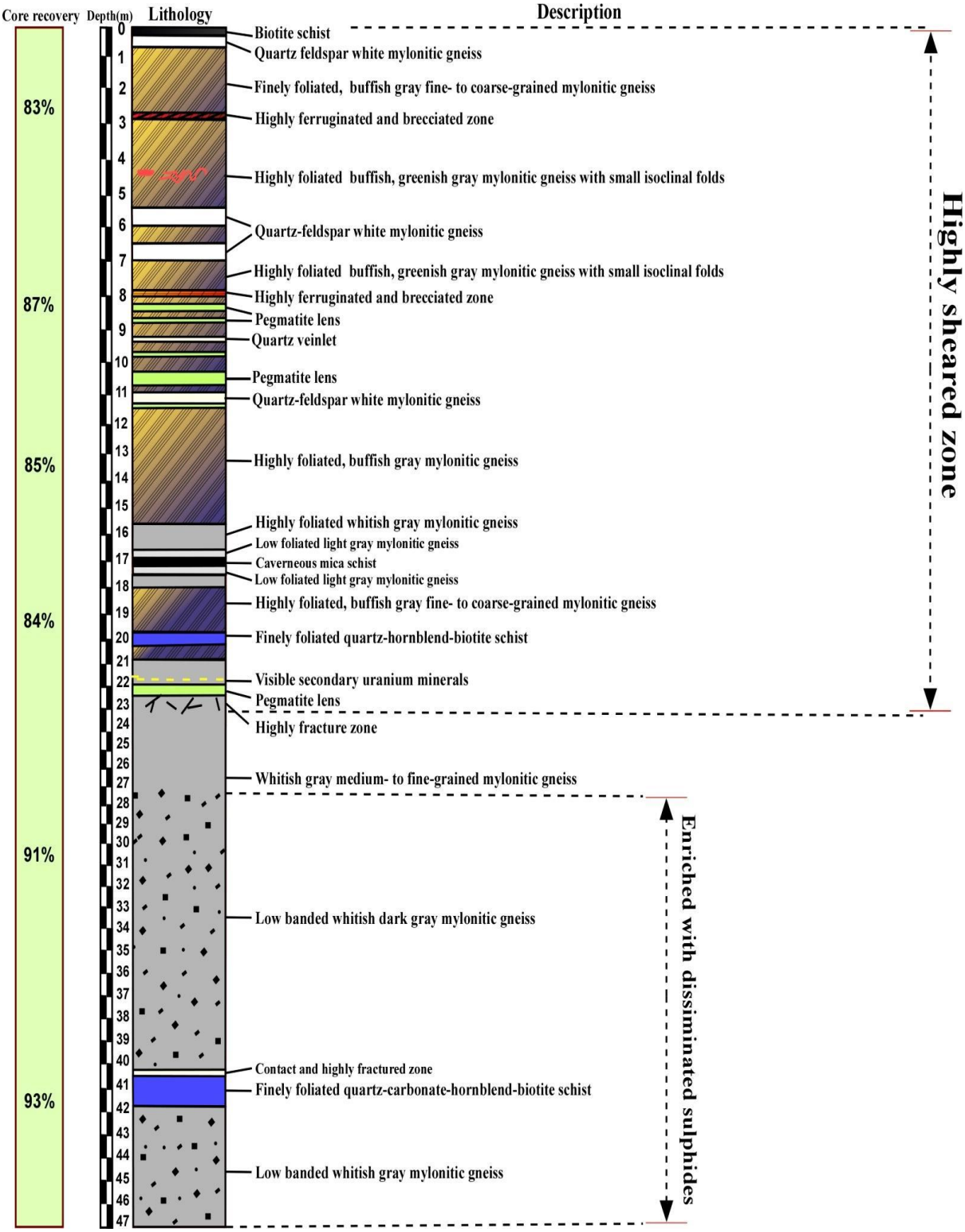

Fig. (3): Lithologic log of the investigated borehole showing the distribution of different lithologic varieties.

Figure 4: Representative photographs of drill core samples from the studied borehole used in this study: a-Mica schist overlies directly quartz feldspar white mylonite gneiss with sharp contact. b- Well-developed millimeter-spaced gneissic banding in buffish gray mylonite gneiss core samples. c- Pegmatite veinlets dissected along the foliation planes and showing isoclinal microfolds in buffish gray mylonite gneiss. d- Brecciation and ferrugination along the fractures. e- Quartz feldspar white mylonite gneiss core sample. f- Quartz-hornblend-biotite schist core sample. g- High foliated whitish gray mylonite gneiss ended by low foliated zone at the contact with caverneous mica schist. h- Caverneous mica schist core sample. i- Dark gray mylonite gneiss core sample. j- Pegmatite core sample. k- Secondary uranium mineralization associating iron. l- Core sample enriched by dissiminated sulphide and black small iron patches. m- Sharp contact between the whitish gray mylonite gneiss and Quartz-carbonate-hornblend-biotite schist. n- Quartz-carbonate-hornblend-biotite schist core sample.

III. Petrographical studies

The gneissic rocks in the borehole are the major category representing about 70% of the borehole and considered as the most important units from the mineralized point of view. This part is devoted to the microscopic investigations of the different lihologic varieties along the studied borehole, handling with the core samples picked from the studied borehole.

Mica-schist is fine- to medium- grained with black color, mainly composed of biotite+ phlogopite±chlorite±opaques. Biotite is the main constituent, occurs in multi-phases as xenomorphic flakes or aggregates of fine flakes with green color arranged in parallel lines in well-defined schistosity (Fig. 3.5a). Phlogopite occurs as stretched and deformed flakes with high interference colors. The rock contains appreciable amount of chlorite, quartz and opaque minerals. **Quartzo-feldspathic white mylonitic gneiss**, the main constituents are quartz and feldspars (including plagioclase and perthite), biotite, zircon and allanite are accessories (Fig. 5b). Plagioclase and quartz occur as oriented euhedral crystals associated with metamectized and non-metamectized zircon and shows directional orientation (Figs. 5c and 5d). T**he buffish gray mylonite gneiss** is composed mainly of quartz, plagioclase, potash feldspar, in addition to fewer amounts of biotite and muscovite (Fig. 5e). Textures are medium- to coarse-grained, gneissic to blastomylonitic. Quartz is the most dominant mineral occurs as subhedral crystals with average size about 0.2mm-2.5 mm; it is also present as elongated porphyroblast. Plagioclase ranges from albite to andesine (An_{28-35}), appears as hypidiomorphic and xenomorphic crystals show cloudy appearance characterized by medium grain size with lamellar and Carlsbad twinning. In this zone, plagioclase is moderately affected by stress represented by breaking, bending and then dislocation. Potash feldspars are mainly represented by porphyroblasts of perthite, occurring as stretched and oriented aggregates of string perthite, patch perthite and flame perthite (Fig. 5f). Mica minerals are present mainly as foliated flakes of biotite with appreciable amount of muscovite. Accessory minerals comprise apatite, zircon, fluorite and opaques. Zircon occurs either as minute crystals included in biotite surrounded by strong pleochroic halos due to radiogenic effect or as euhedral crystals zoned and twinned crystals, (Fig. 5g). The alternating bands of **Quartz-hornblende-biotite schist** is characterized by schistose structure and mainly composed of quartz, biotite, hornblende (Fig. 5h) and some carbonate minerals in quartz-carbonate-hornblend-biotite schist (Fig. 5i). Quartz appears as stretched crystals parallel to the other constituents. Hornblende occurs as subhedral to euhedral foliated crystals, varying from 0.8 to 3.3 mm in length and from 0.2 to 1.5 mm in width. Biotite is present as small flakes, arranged in parallel lines in well-defined schistose structure. Carbonates are present as polygonal aggregates of calcite with extremely high-order interference colors showing abundant twin bands caused by deformation and accumulation of strain especially the polysynthetic twin bands. Finally **whitish gray mylonite gneiss** is moderately foliated, with a well-developed granoblastic-polygonal texture. Locally, mylonitic texture is observed in strongly deformed varieties consist mainly of quartz, K-feldspars, plagioclase, together with biotite and muscovite, (Fig.5j). Accessory minerals are mostly represented by euhedral and highly fractured crystals of zircon with inclusions, monazite. Secondary uranium mineralization is found in this zone of the mylonitic gray gneiss. It occurs as stains along crevices and fracture surfaces and as acicular crystals filling cavities (Figs. 5k). Opaques occur as subhedral to anhedral megacrystals encloses minute crystals of zircon and muscovite (Figs. 5l).

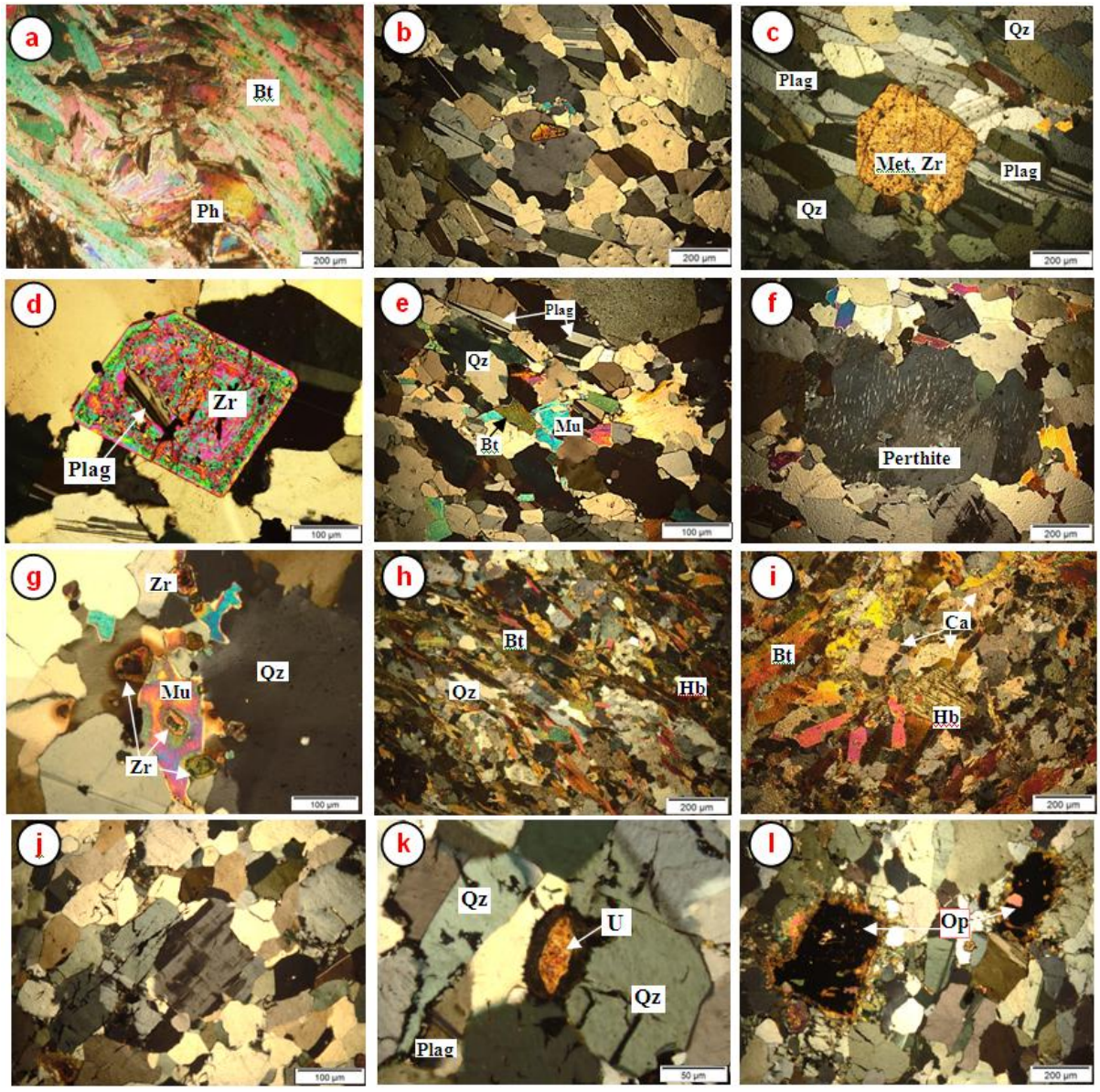

Figure 5: Photomicrographs of drill core samples from the studied borehole showing: a- Foliated flakes of biotite (Bt) and phlogopite (Ph) forming schistose structure (mica schist core sample) CN. b- Band of plagioclase alternating with quartz showing gneissosity (quartz feldspar mylonitic gneiss core sample) CN. c- Alternation of quartzo-feldspathic associating metamectized and fractured zircon crystal, (quartz feldspar mylonitic gneiss core sample) CN. d- Coarse crystal of zircon enclosing minute crystal of p;agioclase (Plg), (quartz feldspar mylonitic gneiss core sample) CN. e- Stretched crystals of quartz, plagioclase, biotite and muscovite forming gneissose texture (buffish gray mylonite gneiss core sample) CN. f- Oriented string perthite crystal (buffish gray mylonite gneiss core sample) g- Group of zircon (Zr) crystals associating muscovite (Mu) with pleochroic halos, (buffish gray mylonite gneiss core sample) CN. h- Schistose structure exhibited by biotite, hornblend and quartz, (quartz-hornblend-biotite schist core sample), CN. i- Quartz, hornblend and biotite associated with calcite (Ca), (quartz-carbonate-hornblend-biotite schist core sample), j- well-developed granoblastic-polygonal texture (whitish gray mylonitic gneiss core sample), CN. k- Secondary uranium (U) associated with iron oxides filling cavity (whitish gray mylonitic gneiss core sample). l- Fragment of opaque (Op) minerals encloses minute crystals of zircon & muscovite, (whitish gray mylonite gneiss), (C.N.).

MINERALIZATION

Based on some polished section of studied drillcore samples from different hole depths were prepared and examined by Environmental Scanning Electron Microscope (ESEM) Phillips EXL 130 and attached by EDX unite system. So Si, Al, Fe and Ca will be increase in the most analysis. All these analysises were carried out on the Laboratories of the Nuclear Materials Authority (NMA), Cairo, Egypt.

3.1 Results and discussions

From a mineralogical point of view, the mylonite gneiss was found to be rich in (a) uranium minerals [Gummite (yttriumuraninite), [uranophane (Ca $(UO_2)_2SiO_3$ (OH)2. 5(H_2O)) and kasolite, $Pb(UO_2)SiO_4(H_2O)$]; (b) thorium minerals [uranothorite, $(Th,U)SiO_4$]; Thorite ($ThSiO_4$), (c) base metals [botryoidal sphalerite (Schalenblende)), Przibramite (cadmiun sphalerite), Galena, Clausthalite (PbSe) and Berzelianite (Cu_2Se)] (d) Nb-Ta minerals [Yttrocolumbite or Samarskit, $(YFe^{3+}Fe^{2+}U,Th,Ca)2(Nb,Ta)2O_8$; fergusonite, $YNbO_4$; Betafite [$(Fe, Ca,Th,U)(Ti,Nb,Ta)O_6$-·$nH_2O$] and pyrochlore $(Pb,Y,U,Ca)2\text{-}xNb_2O_6(OH)$], in addition to zircon, xenotime, monazite, fluorite, and iron oxide minerals (hematite, ilmenite, goethite, and magnetite; Table.1).

A.2. **Gummite (yttriumuraninite)** it's amorphous mixture of natural uranium oxides (uraninite) and secondary uranium minerals of variable composition, representing the final oxidation and hydration stages of uraninite that usually occurs as dense masses and crusts in many of the known uraninite localities (Frondel, C. 1956). Gummite, named in reference to the gum-like appearance or luster of some varieties.

Gummite is recorded for the first time in the studied area that occurs as orange to orange–red subhedral crystals and is usually associated with meta-autunite as yttrogummite and confirmed by SEM, (Fig. 14b).: A yttrium uranium (REE) Contains relatively large amounts of the yttrium earths with significant amounts of Yb and Er, that derived from the alteration of yttriumuraninite. The obtained EDX analysis exhibits that; (U = 52.80 %, Y = 21.66%, Yb = 8.90 % and Er = 4.49%. **Uranophane {Ca $(UO_2)_2SiO_3$ (OH)2. 5(H_2O)}** in the studied borehole, uranophane is the dominant secondary uranium mineral. Cebron et al., (1993) stated that uranophane is a monoclinic uranyl silicate mineral fairly common in the oxidized zone of most deposits. The conditions of formation of this mineral include both the late stages reactions of uraninite with hydrothermal solutions and also alteration by groundwater (Niniger, 1954; Frondel, 1958; Finch and Ewing, 1992). In the studied samples, uranophane found together with pyrite and gummite as massive aggregates. Uranophane mineral exhibits canary yellow to yellow color with dull to greasy luster. ESEM analyses of uranophane (Fig.6b) show that the mineral consists essentially of U (86.12 wt %), Si (3.41 wt %), Ca (6.97 wt %) with the presence of some trace amounts of other elements as K (2.73 wt %) and Al (0.77 wt %). **Kasolite {Pb (UO_2) SiO_4· (H_2O)}** it ranks second in abundance after uranophane and beta-uranophane that is occurred in pegmatites and formed under oxidizing conditions. Maurice (1982) suggested that kasolite is dimorphous with uranophane and beta-uranophane due to the complete replacement of Ca by Pb during the high degree of oxidation condition. The studied kasolite occur as thin flakes with reddish yellow to brownish yellow with vitrous luster and characterized by conchiodal fractures as detected by ESEM (Fig.6c). **Betafite [$(Fe,Ca,Th,U)(Ti,Nb,Ta)O_6$·$nH_2O$]** is a mineral group in the pyrochlore supergroup. Betafite is an important ore of thorium, uranium, and niobium. Lumpkin and Ewing (1996), Turner (1928) and many others are all with the recurring theme of extracting uranium, thorium, and niobium from the pyrochlore super-group ores. It is found as an alteration phase, very dark in color, containing potential concentrations of the high-field-strength elements (HFSE), such as Ti, Nb, and Ta, besides U; these were obtained by SEM-BSE images, (Fig. 6d).

Botryoidal sphalerite (Schalenblende) This mineral is the chief ore of zinc. It consists largely of zinc sulfide in crystalline form but almost always contains variable iron. It is occurring as Oolitic forms with concentric layers around a nucleus with reniform surfaces which also contain intergrown, uranium, cadmium, pyrite and selenium showing botryoidal or ring-like structures. It is believed to have formed by relatively rapid crystallization of a low temperature sulfide gel (gel: colloidal dispersion). It is noteworthy that sphalerite content increases with increasing depth particularly in whitish gray mylonitic gneiss that occurs associated with pyrite, galena, fluorite, monazite, zircon and yttriumuraninite confirmed by SEM, (Fig. 6e). **Przibramite (Zn, Cd) S** is a recognized variety of cadmiferous sphalerite with up to 2% Cd, described firstly in the locality of Przibram. The Cd content of sphalerite depends on the Cd/Zn ratio, ligand activities, and temperature of the ore forming fluids (Michel, 2000). The geochemical cycle of cadmium follows closely that of zinc. The distribution of Cd and Zn between liquid and a solid phase with the end member compositions CdS and ZnS is described by the following equilibrium (Mookherjee, 1962; Tsusue and Holland, 1966; Sverjensky, 1985): ZnS (s)+Cd^{+2} (aq) = CdS(s)+Zn^{+2}(aq). It is found together with pyrite, botryoidal sphalerite and yttriumuraninite and confirmed by SEM (Fig. 6f). **Galena** (PbS) also called lead glance, is the natural mineral form of lead sulfide It is the most important ore of lead and an important source of silver. Galena is one of the most abundant and widely distributed sulfide minerals. It crystallizes in the cubic crystal system often showing octahedral forms. It is found as dissemination usually coexisting with the minerals sphalerite, pyrite and chalcopyrite and confirmed by SEM, (fig. 6g).

Selenium minerals, in 1956, Thompson et al. discovered felty native selenium, which is violet acicular crystal. Coleman and Delevaux (1957) investigated the occurrence of selenium in sulphide from sandstone-type uranium ores in the western USA, and discovered trigonal and monoclinic native selenium, as well as clausthalite and ferroselite (Thompson et al,. 1956; Coleman and Delevaux, 1957). The occurrence of large particle of native selenium up to 20-30 mm in length in coal seams was reported by Zhu et al., (2005). In 1990, spherical and

tubular native selenium was discovered in a hydrothermal U-Se-Re polymetallic deposit (Zhu et al., 2003). **Clausthalite** (**PbSe**) is a lead selenide mineral, it is also considered as the first recording in the study area. It occurs in low-sulfur hydrothermal deposits with other selenides. It is used as a very minor ore of lead and selenium. Clausthalite is a member of the Galena Group of minerals. Its properties are very similar to galena as it shares basically the same structure. However it can be distinguished from the far more common galena by its greater density and lack of good crystals. The two minerals are in a series in which the sulfur and selenium ions substitute for each other. Clausthalite occurs mainly as finer particles in the size range from 0.005 mm to 0.01 mm, it is often closely associated with other minerals The ESEM analyses of the studied Clausthalite are shown in (fig. 6h). **Berzelianite** is a rare copper selenide mineral with the formula **Cu_2Se**. It occurs in small, distinct particles dispersed in matrix. Berzelianite often occurs together with Clausthalite, pyrite, sphalerite and yttriumuraninite. The ESEM analyses of Berzelianite crystals indicate the deposition of Berzelianite over pyrite crystals (Fig. 6g). Clausthalite and Berzelianite are considered as the first recording in the study area.

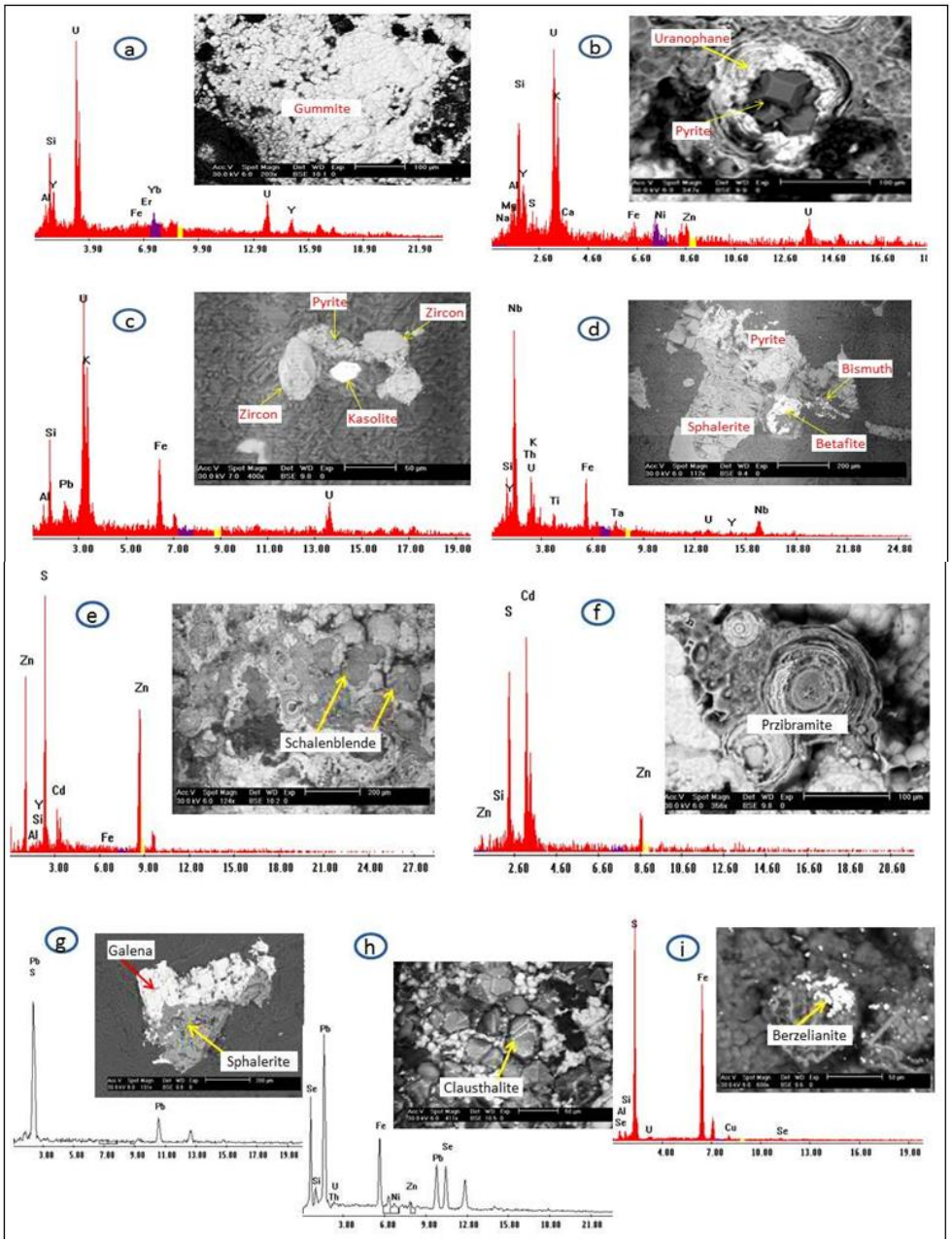

Fig. 6: Back Scattered Electron images and spectrum showing: a- Gummite mineral. b- Uranophane mineral associating pyrite. c- Kasolite mineral. d- Betafite associating base metals. e- Botryoidal sphalerite (Schalenblende). f- Przibramite mineral. g- Galena coexisting with sphalerite. h- Clausthalite mineral. i- Berzelianite mineral

Table 1: Minerals recovered in the mineralized samples of the studied borehole, Abu Rusheid area, SED, Egypt.

Mineral group	Minerals
Uranium minerals	Gummite (yttriumuraninite) (first recording), uranophane, and kasolite.
Thorium	Thorite and Uranothorite.
Base metals	Sphalerite, galena, pyrite, chalcopyrite, Przibramite, Clausthalite and Berzelianite.
Nb-Ta minerals	Pyrochlore, betafite, and fergusonite.
Accessory minerals	Zircon, xenotime, monazite and fluorite.
Iron minerals	Hematite, ilmenite, goethite, and magnetite.

4. RADIOACTIVE MEASUREMENTS

Laboratory procedures: Twenty-five representative core samples of the different levels were collected for laboratory studies. The radiometric measurements were carried out on these core samples from the drilled borehole. The results are given in table (2). Equivalent [U] and [Th] concentrations are measured radiometrically by using multi-channel analyzer Gamma-ray detector (Gamma-spectrometer technique). The studied core samples were crushed well to small size (-60 mech) using mechanical crusher. Then the crushed rocks were dried to very small levels of humidity,mixed well and the representative crushed rock sample (250 – 300 gm) was put into circuler plastic containers with diameter nearly equal 10 cm and 3 cm in height. Every sample then was pressed manually in the prepared containers till it was completely filled and tightly closed. The prepared samples were stored for about 30 days to reach the equilibrium state and accumulate free Radon gas. The measurements are expressed in [ppm] for eU & eTh and percent for K. Radioactivity were measured then related to the standards for U, Th and K provided by International Atomic Energy Agency (IAEA).

4.2 Results and discussions

In the studied borehole, the uranium and thorium contents of buffish, greenish mylonitic gneiss samples is medium where the eU ranged from 51 to 102 ppm with an average 80.7 ppm and the eTh content vary from 100 to 504 ppm with an average 241 ppm. The (eTh/eU) ratio ranged from 1.5 to 4.9 with an average 2.9. This relation between both eU and eTh indicates that the content of eTh more than the content of eU this is regarded to the presence of thorium bearing minerals observed in mineralogical examination. while the uranium and thorium contents of Whitish gray mylonitic gneiss samples is high where the eU ranges from 68 to 179 ppm with an average 147 ppm and the eTh content varies from 155 to 467 ppm with an average 253ppm. The (eTh/eU) ratio ranged from 0.9 to 2.8 with an average 1.8 as well as thorium content at this zone represents the highest thorium content along the borehole except at depth 24m where the uranium content more than thorium content (eU=179ppm, eTh=155ppm) this is also regarded to the presence of observable secondary uranium. In addition to, the uranium and thorium contents of the quartz feldspar white mylonitic gneiss and dark gray mylonitic gneiss are lower than the previous mylonitic gneissic types while the schistose rock types represent the lowest values along the studied borehole

Fig (7) shows the distribution and variation of eU, eTh and eTh/eU ratio with depth at the studied borehole, also, we can notice the following:

1- More than one radioactive anomaly are detected and the highest two zones is related to whitish gray mylonitic gneiss of the studied borehole at different depths. 2- These radioactive anomalies are related mainly to uranium and thorium concentrations but thorium concentration more than uranium concentration along the borehole. 3-The positive anomalies of uranium correspond to positive thorium anomalies and positive Th/U ratio and there is a general trend for increasing of uranium and decreasing thorium with depth for the studied borehole.

Table (2): Radiometric analyses (ppm) for the subsurface core samples of the studied borehole

Rock type	Buffish, greenish mylonitic gneiss				Quartz-feldspar white mylonitic gneiss		Buffish, greenish mylonitic gneiss					Whitish gray mylonitic gneiss	
Depth(m)	1	2	3	5	6	7	10	12	15	20	Average	16	18
eU	102	68	92	75	65	56	87	79	51	92	80.7	160	173
eTh	504	324	170	289	148	168	193	203	100	141	241	354	213
eTh/eU	4.9	4.8	1.8	3.8	2.3	3	2.2	2.6	1.96	1.5	2.9	2.2	1.24

Continue:

Rock type	Whitish gray mylonitic gneiss								Dark gray mylonitic gneiss				Schistose rocks	
Depth(m)	24	26	28	29	41	43	45	Average	33	35	36	38	Average	20	42
eU	179	127	116	170	156	175	68	147	100	92	67	57	79	16	12
eTh	155	237	193	467	191	266	197	253	116	253	132	134	158	37	28
eTh/eU	0.9	1.9	1.6	2.7	1.2	1.5	2.8	1.8	1.16	2.7	1.97	2.3	2.05	2.3	2.3

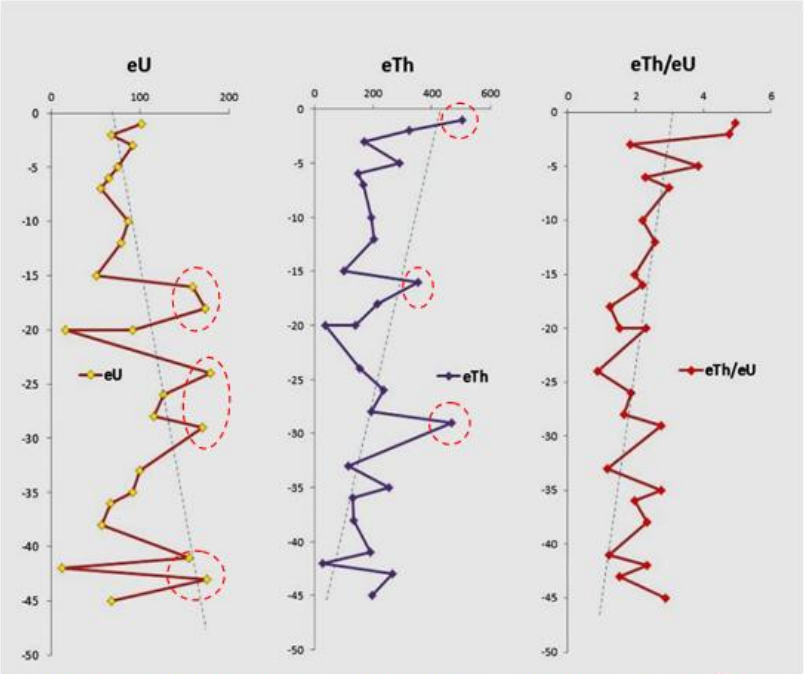

Fig. (7): eU, eTh (ppm) and (eTh/eU) ratio with depth of the studied borehole ( ) Anomaly).

V. Conclusion

The underlying metamorphic units in the studied borehole are lithologically represented mainly (from top to bottom) by mica schist, buffish gray mylonite gneiss, quartz feldspar whitish mylonite gneiss, caverneous mica schist, quartz-hornblend-biotite schist and finally whitish gray mylonite gneiss interrupted by thin layer of quartz-carbonate-hornblend-biotite schist.

The detailed mineralogical studies proved that; the yttriumuraninite (gummite), uranophane, are found together with botryoidal sphalerite (with colloform texture), Przibramite ((Zn,Cd)S), Clausthalite (PbSe) and Berzelianite (Cu_2Se) as well as well-developed pyrite. The previous assemblage recorded for the first time in the area under investigation, in addition to radioactive minerals comprising primary uranium mineral such as uranothorite, secondary uranium minerals such as uranophane and kasolite as well as rare metal mineral species such thorite, niobium minerals (columbite, pyrochlore, betafite, samarskite and fergusonite), xenotime, zircon and monazite.

The radiometric analysis showed that, the whitish gray mylonitic gneiss samples represent the highest radioactive zone. The radioactivity is related mainly to uranium and thorium concentrations**.** Also, there is a general trend for increasing of uranium and decreasing thorium with depth for the studied borehole.

References

[1]. Abd El-Naby and H., Frisch, W., (2006): Geochemical constraints from the Hafafit Metamorphic Complex (HMC): evidence of Neoproterozoic back-arc basin development in the central Eastern Desert of Egypt. Journal of African Earth Science, 45, 173-186.
[2]. Abd El-Naby, H. and Frisch, W., (2002): Origin of the Wadi Haimur–Abu Swayel Gneiss belt, South Eastern Desert, Egypt: Petrological and geochronological constraints, Precambrian Research, 113: 307 322.
[3]. Abd El-Naby, H., Frisch, W., Hegner, E., (2000): Evolution of Pan-African Wadi Haimur metamorphic sole, Eastern Desert, Egypt. Jounal of Metamorphic Geology, 18, 639-651.
[4]. Assaf, H. S., Ibrahim, M. E., Zalata, A. A., El- Metwally, A. A. and Saleh, G. M. (2000): Polyphase folding in Nugrus-Sikeit area south Eastern Desert, Egypt. JKAW: Earth Sci., 12, 1-16 p.
[5]. Cebron, F., Ildefonse, P., and Sichere, M. C., (1993): New mineralogical data on uranophane and B-uranophane, synthesis of uranophane. Mineralogical Mag., 57, pp. 301-308.
[6]. Coleman, R.G. and Delevaux, M.H. (1957): Occurrence of selenium in sulfides from some sedimentary rocks of the western United States. Economic Geology, vol. 52, no. 5. pp. 499-527.
[7]. Finch, R. J. and Ewing, R. C., 1992: The corrosion of uraninite under oxidizing conditions. J. Nucl. Mater. Vol. 190, pp. 133 – 156.
[8]. Fowler, A. and Osman, A. F., (2009): The Sha'it-Nugrus shear zone separating central and south Eastern Deserts, Egypt: A post-arc collision low-angle normal ductile shear zone, Journal of African Earth Sciences, 53: 16-32.
[9]. Fritz, H., Wallbrecher, E., Khudeir, A. A., Abu El-Ela, F. F., and Dallmeyer, D. R., (1996): Formation of Neoproterozoic metamorphic core complexes during oblique convergence Eastern Desert, Egypt. J. African Earth Sci., 23, 311–329.
[10]. Frondel, C. (1956): The mineralogical composition of gummite. American Mineralogist: 41: 539-568.
[11]. Frondel, C., (1958): Systematic mineralogy of uranium and thorium. U.S. Geol. Surv., Bull. 1064:400.
[12]. Greiling, R. O., Kr¨oner, A., El-Ramly, M. F., and Rashwan, A. A., (1988): Structural relations between the southern and central parts of the Eastern Desert of Egypt: details of a fold and thrusts belt. In: El-Gaby, S., Greiling, R. (Eds.).The Pan-African Belt of

the NE Africa and Adjacent Areas.Tectonic Evolution and Economic Aspects.Freidr.Vieweg&Sohn, Braunschweig/Weisbaden, 121-145.

[13]. Ibrahim, M. E.,Saleh, G. M.,Abd El Naby, H. H. Mahmoud, F. O. Abu El Hassan, E. A. Ibrahim, I. H. Aly, M. A., Azab, M. S. Rashed. M. A, Khaleal, F. M. and Mohamed, A. M., (2002): Uranium and associated rare metals potentialities of Abu Rusheid brecciated shear zone, south Eastern Desert, Egypt. (Internal Report) Part I.

[14]. Ibrahim, M. E., Saleh, G. M, Amer, T., Mahmoud, F. O, Abu El Hassan, A. A., Ibrahim, I. H., Aly, M. A., Azab, M. S., Rashed, M. A., Khaleal, F. M. and Mahmoud, M. A., (2004): Uranium and associated rare metals potentialities of Abu Rusheid brecciated shear zone II, south Eastern Desert, Egypt. (Internal report).

[15]. Kröner, A., Greiling, R.O., Reischmann, T., Hussin, I.M., Stern, R.J., Durr, S., Kruger, J., Zimmer, M., (1987): Pan-African crustal evolutionin the Nubian segment of northeast Africa. In: Kro¨ner, A. (Ed.), Proterozoic Lithospheric Evolution, Geodynamics Series, vol. 17. American Geophysical Union, pp. 237–257.

[16]. Lang, A. H., Griffith, J. W. and Steach, H. R., (1962): Canadian deposits of uranium and thorium: Canada Geol. Survey, Econ. Geol. Ser. no. 18, 324 p.

[17]. Lumpkin, G.R., and Ewing, R.C., (1996): Geochemical alteration of pyrochlore group minerals: Betafite subgroup. American Mineralogist, 81, 1237-1248.

[18]. Mahmoud, A. M., (2009): Highlight on the geology, geochemistry and spectrometry of the muscovite granites at Wadi El Gemal area, South Eastern Desert, Egyp. Ph.D. Faculty of science, Suezcanal University.

[19]. Maurice, Y. T., 1982: Uraniferous granite and associated mineralization in the Fury and Hecla Strait area, Baffin Island, N.W.T. In "uranium in granite" paper 81–23. Proceedings of a workshop held in Ottawa, Ontario, 25–26 November. 1980. pp 101-115.

[20]. Michael, O. Schwartz (2000): Cadmium in Zinc Deposits: Economic Geology of a Polluting Element: International Geology Review, 42:5, 445-469

[21]. Mookherjee, A., (1962): Certain aspects of the geochemistry of cadmium: Geochim. et Cosmochim. Acta, v. 26, p. 351-360.

[22]. Niniger, R. D., (1954): Minerals for Atomic Energy: a guide to exploration for uranium, thorium and beryllium. D. van Nostrand Company Inc., Toronto, p259.

[23]. Saleh, G. M. (1997): The potentiality of uranium occurrences in Wadi Nugrus area, southeastern Desert, Egypt. Ph. D. Thesis Mans. Univ. 171 p.

[24]. Sverjensky, D. A., (1985): The distribution of divalent trace elements between sulfides, oxides, silicates and hydrothermal solutions: I. Thermodynamic basis: Geochim. et Cosmochim. Acta, v. 49, p. 853-864.

[25]. Thompson, M., Roach, C., and Braddock, W. (1956): New occurrences of native selenium. American Mineralogist, vol. 41. pp. 156-157.

[26]. Tsusue, A., and Holland, H. D., (1966): The eoprecipitation of cations with CaCO3-III. The eoprecipitation of Zn2+ with calcite between 50 and 250°C: Geochim. et Cosmochim. Acta, v. 30, p. 439-453.

[27]. Turner, H.W., (1928): Review of the Radioactive Minerals of Madagascar. Economic Geology, 23, 62-84.

[28]. Whittle, A.W.G. (1960): Contact mineralization phenomena at the Mary Kathleen uranium deposit. Neues Jahrb. Mineral. Abh., 94_, 798-830.

[29]. XU, G., WANG, A., GU, Q., ZHANG, J., ZHANG, Z. and HUANG, Y. (1981): Some Characteristics of Uranium Oxides in China. Bull. Mineral, v.104, pp.565-574.

[30]. Zhu, J. and Zheng, B. et al., (2005): Morphology features and genesis of native selenium. Bulletin of Mineralogy, Petrology and Geochemistry, vol. 19, no. 4. pp. 353-355 (in Chinese).

[31]. Zhu, J., Liang, X., Qang, M., Wang, F., Ling, H., and Liu, S. (2003): Advances in studying occurrence modes of selenium in environment. Bulletin of Mineralogy, Petrology and Geochemistry, vol. 22, no. 1. pp. 75-81 (in Chinese).

Ahmed S. Shalan. "A new occurrence of yttriumuraninite, Selenium minerals, Sphalerite and Pyrite assemblages from research drilling at Abu Rusheid uranium mineralization, southern Eastern Desert, Egypt.." *IOSR Journal of Applied Geology and Geophysics (IOSR-JAGG),* 9(3), (2021): pp 15-27.